Macroscopic magnetic structures with balanced gain and loss

J. M. Lee and T. Kottos
Department of Physics, Wesleyan University, Middletown, Connecticut 06459, USA

B. Shapiro
Technion–Israel Institute of Technology, Technion City, Haifa 32000, Israel

(Received 14 August 2014; revised manuscript received 21 February 2015; published 17 March 2015)

We investigate magnetic nanostructures with balanced gain and loss and show that such configurations can result in a new type of dynamics for magnetization. Using the simplest possible setup consisting of two coupled ferromagnetic films, one with loss and another one with a balanced amount of gain, we demonstrate the existence of an exceptional point where both the eigenfrequencies and eigenvectors become degenerate. This point corresponds to a particular value of the gain and loss parameter $\alpha = \alpha_c$. For $\alpha < \alpha_c$ the frequency spectrum is real, indicating stable dynamics, while for $\alpha > \alpha_c$ it is complex, signaling unstable dynamics which is, however, stabilized by nonlinearity.

DOI: 10.1103/PhysRevB.91.094416 PACS number(s): 75.75.−c, 05.45.Xt, 11.30.Er, 76.50.+g

I. INTRODUCTION

Spin dynamics in synthetic magnetic nanostructures has attracted increasing attention during the last few years [1] because of the interesting fundamental physics involved and also because of its important practical applications: magnetic storage and information processing [2,3], sensing [4], and creation of tunable high-frequency oscillators [5] are some of the areas that have benefited from this research activity. An important step in this endeavor is the realization of new magnetic nanodevice architectures with additional degrees of freedom which permit better control of magnetization dynamics.

Along the same lines, management of classical wave propagation via synthetic structures has been proven to be successful, resulting in the creation of new materials with unexpected properties. Examples of this success include the realization of metamaterials which exhibit phenomena like cloaking, negative index of refraction, etc. The operation frequency for many of these proposals spans a wide range from optics [6] and microwaves [7] to acoustics [8]. Quite recently, a new type of synthetic structure which possesses spatiotemporal reflection symmetry, or parity-time ($\mathcal{PT}$) symmetry, has emerged. These structures are implemented using judicious manipulation of loss and gain mechanisms [9–21]. Their spectra undergo a transition from real to complex once the parameter that controls the degree of gain and loss in the system reaches a critical value [22]. The transition point shows the characteristic features of an *exceptional point* (EP), where both eigenfrequencies and normal modes coalesce. For values of the gain and loss parameter which are smaller than the critical value the eigenvectors of the equations of motion are also eigenvectors of the $\mathcal{PT}$ operator, while above the critical value, they cease to be eigenvectors of the $\mathcal{PT}$ operator. The former domain is termed the *exact phase*, while the latter is the *broken phase*. This terminology is borrowed from the "$\mathcal{PT}$-symmetric quantum mechanics" community (see the review in [23]). One should keep in mind, however, that the systems studied in [9–21] are purely classical, with loss and gain being introduced on a phenomenological level, and as such, they are quite different from the $\mathcal{PT}$-symmetric quantum systems envisaged by Bender and collaborators [23].

The resulting wave structures show several intriguing features such as power oscillations [9–13], nonreciprocity of wave propagation [14–16], unidirectional invisibility [11,17–19], and coherent perfect absorbers and lasers [20]. Experimental realizations have been reported in the framework of optics [10,11,16,17,21] and electronic circuitry [12,15,18], while the applicability of these ideas has been theoretically demonstrated in Bose-Einstein condensates [24] and in acoustics [25].

In this paper we propose a class of synthetic magnetic nanostructures which utilize natural dissipation (loss) mechanisms together with judiciously balanced amplification (gain) processes in order to control magnetization dynamics. Amplification in such structures can be achieved with the help of certain external factors such as parametric driving or spin-transfer torque (see Sec. V), while loss comes from coupling with the phonons or other degrees of freedom. As a prototype system we consider two ferromagnetic films (see Fig. 1), one with loss and the other with an equal amount of gain, coupled by an exchange or by a dipole-dipole interaction. The magnetization dynamics is described in terms of two vector variables, the macroscopic magnetic moments of each film, whose evolution is given by the nonlinear Landau-Lifshitz-Gilbert equations. We will demonstrate that despite the fact that the system is non-Hermitian, if the gain and loss parameter is below a critical value, the macroscopic magnetic moments precess about the direction of an effective magnetic field inside the sample without being amplified or attenuated. Specifically, below a critical value of the gain and loss parameter, the eigenfrequencies of the linearized Landau-Lifshitz-Gilbert equations are real, while above this critical value, they become complex, leading to dynamical instabilities that are limited only by nonlinear effects. The transition point is characterized by an EP degeneracy. Our proposal reveals a new type of steady-state dynamics which could be useful for manipulating magnetization switching and could potentially lead to new device design. Moreover, the realization of EP degeneracies may be utilized for enhanced sensitivity in sensing via frequency splitting [26].

The structure of this paper is as follows. In Sec. II we present the mathematical model that describes our system. It consists of two coupled nonlinear Landau-Lifshitz-Gilbert

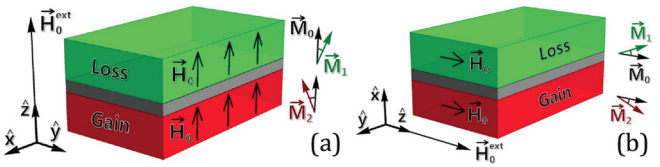

FIG. 1. (Color online) Two coupled ferromagnetic films in the presence of an external magnetic field which is along the z axis. We distinguish between two geometries: (a) out-of-plane geometry (the z axis is perpendicular to the films) and (b) in-plane geometry (the z axis is parallel to the films).

(LLG) equations. In Sec. III we investigate the out-of-plane geometry. In Sec. III A we analyze the eigenfrequencies and the eigenmodes of the linearized LLG equations for different values of the gain and loss parameter. The dynamics generated by the $\mathcal{PT}$-symmetric LLG equations and its comparison to the results from the linearized LLG equations are discussed in Sec. III B. In Sec. IV we analyze an in-plane (magnetization) geometry. Finally, in Sec. V we discuss two different physical mechanisms which allow us to incorporate and manage gain in a magnetic nanostructure. Our conclusions are given in Sec. VI.

II. MATHEMATICAL MODELING

We consider two ferromagnetic films $n = 1,2$ separated by a nonmagnetic layer. The two geometries that we will consider here are shown in Fig. 1. In Fig. 1(a), we assume a uniform external magnetic field $\vec{H}_{\rm ext}$ perpendicular to the plane of the films (out-of-plane geometry), while in Fig. 1(b) the external field is parallel to the films (in-plane geometry). The magnetization within each film is uniform and is represented by a magnetic vector $\vec{M}_{n=1,2}$. When the magnetic configuration is away from equilibrium the magnetization precesses around the instantaneous local effective field $\vec{H}_n$. The latter is generally a complicated function of $\vec{M}_n$ and the external magnetic field $\vec{H}_{\rm ext}$. For the cases shown in Fig. 1 we have

$$\vec{H}_n = \vec{H}_{\rm ext} - 4\pi \hat{N}\vec{M}_n, \tag{1}$$

where the demagnetizing tensor $\hat{N}$ takes the simple form $\hat{N}_{i,j} = \delta_{i,3}\delta_{j,3}$ for the out-of-plane geometry and $\hat{N}_{i,j} = \delta_{i,1}\delta_{j,1}$ for the in-plane geometry ($i,j = 1,2,3$ indicates the $\hat{x},\hat{y},\hat{z}$ directions, respectively).

The time evolution of the magnetization dynamics for this coupled system can be described by a pair of coupled modified LLG equations:

$$\begin{aligned}
\frac{\partial \vec{M}_1}{\partial t} &= -\gamma \vec{M}_1 \times \vec{H}_1 - \gamma K \vec{M}_1 \times \vec{M}_2 + \frac{\alpha}{|\vec{M}_1|}\vec{M}_1 \times \frac{\partial \vec{M}_1}{\partial t},\\
\frac{\partial \vec{M}_2}{\partial t} &= -\gamma \vec{M}_2 \times \vec{H}_2 - \gamma K \vec{M}_2 \times \vec{M}_1 - \frac{\alpha}{|\vec{M}_2|}\vec{M}_2 \times \frac{\partial \vec{M}_2}{\partial t},
\end{aligned} \tag{2}$$

where γ is the gyromagnetic ratio. The first term on the right-hand sides of Eqs. (2) describes the interaction of the magnetization $\vec{M}_n$ of each layer with the corresponding local field $\vec{H}_n$. The second term represents the coupling between the two ferromagnetic layers. We assume ferromagnetic coupling, i.e., $K > 0$. The last term of the first equation describes dissipation processes and can be introduced in the original LLG equations by assuming that an effective local friction is pushing the magnetic moment $\vec{M}_1$ towards the direction of the effective magnetic field acting on that moment. It was introduced by Gilbert in order to describe dissipation and can be shown to be equivalent to the term that was proposed originally by Landau and Lifshitz for the same purpose [1]. The parameter α is the Gilbert damping term. The last term of the second equation is similar, but the sign is reversed, reflecting the possibility of amplification mechanisms. We discuss experimentally realizable ways to achieve "gain" in Sec. V.

For $\alpha = 0$, Eqs. (2) are invariant with respect to the interchange $\vec{M}_1 \leftrightarrow \vec{M}_2$. Notice that this interchange implies also an interchange of $\vec{H}_1 \leftrightarrow \vec{H}_2$ via Eq. (1). We refer to this symmetry as the "parity" ($\mathcal{P}$) symmetry. When $\alpha \neq 0$, the parity symmetry of our system is destroyed. However, Eqs. (2) are still invariant under a *combined* parity $\mathcal{P}$ and time reversal $\mathcal{T}$ operation. The latter corresponds to a time inversion $t \to -t$ together with a simultaneous change of the sign of all pseudovectors, i.e., $\vec{M}_n \to -\vec{M}_n$ and $\vec{H}_n \to -\vec{H}_n$. This definition of the time-reversal operation is necessary when magnetic fields, which break the time reversibility in a Hermitian manner, are present. Finally, we note that all terms in Eqs. (2) conserve the length of the magnetization vectors $\vec{M}_n$. This can be easily seen by taking the inner product of each of the above equations with the respective $\vec{M}_n$. This yields $\vec{M}_n \frac{\partial \vec{M}_n}{\partial t} = \frac{1}{2}\frac{\partial \vec{M}_n^2}{\partial t} = 0$, indicating that $|\vec{M}_n|$ are constants of motion.

Below, we first analyze the parametric evolution of the eigenfrequencies and normal modes associated with small oscillations around the equilibrium configuration as the gain and loss parameter α increases. To this end, we separate the magnetization of each film into its equilibrium value, which is assumed to be the same for both films, $\vec{M}_n^{(0)} = \vec{M}^{(0)}$, and its oscillating part $\vec{m}_n$, i.e., $\vec{M}_n = \vec{M}^{(0)} + \vec{m}_n$, where $|\vec{m}_n| \ll |\vec{M}^{(0)}|$. Furthermore, the external magnetic field can be decomposed into its constant value $\vec{H}_{\rm ext}^{(0)}$ and a time-dependent part $\vec{h}_{\rm ext}$, i.e., $\vec{H}_{\rm ext} = \vec{H}_{\rm ext}^{(0)} + \vec{h}_{\rm ext}$. In Sec. III we focus on the out-of-plane geometry [see Fig. 1(a)], while in Sec. IV we briefly discuss the in-plane geometry [see Fig. 1(b)].

III. OUT-OF-PLANE GEOMETRY

A. Linearized LLG equations and parametric evolution of their normal modes

For the out-of-plane geometry we recall relation (1), which allows us to connect the external field $\vec{H}_{\rm ext}$ to the local internal field $\vec{H}_n$. Linearizing Eqs. (2) with respect to $\vec{m}_n$ and, furthermore, setting $\vec{h}_{\rm ext} = 0$, we obtain the following linear set of equations:

$$\begin{aligned}
\frac{\partial \vec{m}_1}{\partial t} &= (\omega_H + \omega_K)\hat{z} \times \vec{m}_1 - \omega_K \hat{z} \times \vec{m}_2 + \alpha \hat{z} \times \frac{\partial \vec{m}_1}{\partial t},\\
\frac{\partial \vec{m}_2}{\partial t} &= (\omega_H + \omega_K)\hat{z} \times \vec{m}_2 - \omega_K \hat{z} \times \vec{m}_1 - \alpha \hat{z} \times \frac{\partial \vec{m}_2}{\partial t},
\end{aligned} \tag{3}$$

where $\omega_K = \gamma K|\vec{M}_0|$ and $\omega_H = \gamma|\vec{H}_0|$. Here $|\vec{H}_0| = |\vec{H}_{\rm ext}^{(0)}| - 4\pi|\vec{M}_0|$ is the constant internal magnetic field, which is assumed to be the same for both films.

Assuming a harmonic time dependence for the magnetization $\vec{m}_n(t) = \vec{m}_n \exp(-i\omega t)$, we have

$$-i\omega\vec{m}_1 = (\omega_H + \omega_K - i\alpha\omega)\hat{z}\times\vec{m}_1 - \omega_K\hat{z}\times\vec{m}_2,$$
$$-i\omega\vec{m}_2 = (\omega_H + \omega_K + i\alpha\omega)\hat{z}\times\vec{m}_2 - \omega_K\hat{z}\times\vec{m}_1. \quad (4)$$

Note that, although formally $\vec{m}_1$ and $\vec{m}_2$ are three-dimensional vectors, only the transverse (x,y) components appear in a nontrivial manner. The longitudinal components m_{1z} and m_{2z} are zero in the linear approximation, as follows from Eqs. (4). This is a straightforward consequence of the already mentioned constraint of the strictly conserved length of vectors $\vec{M}_1$ and $\vec{M}_2$. Thus, the magnetic vectors have only two independent components, and if the transverse components are known, the longitudinal component can be found from the constraint. When $\vec{m}_1$ is treated in the linear approximation, then $m_{1z} = -m_1^2/2|\vec{M}^{(0)}|$ (and similarly for m_{2z}). In Sec. III B, where the exact nonlinear dynamics is treated, we use spherical coordinates, which makes it manifestly clear that there are only two independent degrees of freedom (two angles) for each magnetic moment.

The analysis of Eqs. (4) can be simplified by using the "center-of-mass" coordinates of the system. We define $\vec{\Delta} \equiv \vec{m}_1 - \vec{m}_2$ and $\vec{\mu} \equiv \vec{m}_1 + \vec{m}_2$. Then Eqs. (4) take the following form:

$$[(1+\alpha^2)\omega^2 - (\omega_H + 2\omega_K)^2]\vec{\Delta} + 2i\alpha\omega(\omega_H + \omega_K)\vec{\mu} = 0,$$
$$2i\alpha\omega(\omega_H + \omega_K)\vec{\Delta} + [(1+\alpha^2)\omega^2 - \omega_H^2]\vec{\mu} = 0, \quad (5)$$

which allows us to decouple the x and y components of the center-of-mass coordinates $\vec{\Delta},\vec{\mu}$. Thus, the original set of four coupled equations reduces to two uncoupled sets for the x and y components, respectively.

The eigenvalues and the normal modes can be found by solving the 2×2 secular equation for one of these components. The eigenfrequencies are given by

$$\omega_{1,2} = \frac{\omega_H + \omega_K \pm \sqrt{\omega_K^2 - \alpha^2\omega_H(\omega_H + 2\omega_K)}}{1+\alpha^2}. \quad (6)$$

The limiting case of $\alpha = 0$ results in two eigenfrequencies: (a) $\omega_1 = \omega_H$, associated with the "soft" mode (frequency approaches zero when $|\vec{H}_0| \to 0$), with $\vec{m}_1 = \vec{m}_2$, and (b) $\omega_2 = \omega_H + 2\omega_K$, associated with the "hard" mode, with $\vec{m}_1 = -\vec{m}_2$. As the gain and loss parameter α increases, the two eigenfrequencies approach one another (see Fig. 2), and at some critical value $\alpha = \alpha_{\rm cr}$ they coalesce and bifurcate into the complex plane. Using Eq. (6) we calculate the critical frequency $\omega_{\rm cr}$ and the critical value of the gain and loss parameter to be

$$\alpha_{\rm cr} = \frac{\omega_K}{\sqrt{\omega_H(\omega_H + 2\omega_K)}}, \quad \omega_{\rm cr} = \frac{\omega_H(\omega_H + 2\omega_K)}{\omega_H + \omega_K}. \quad (7)$$

Near the phase-transition point $\alpha_{\rm cr}$, the eigenfrequencies display the characteristic behavior of an exceptional point

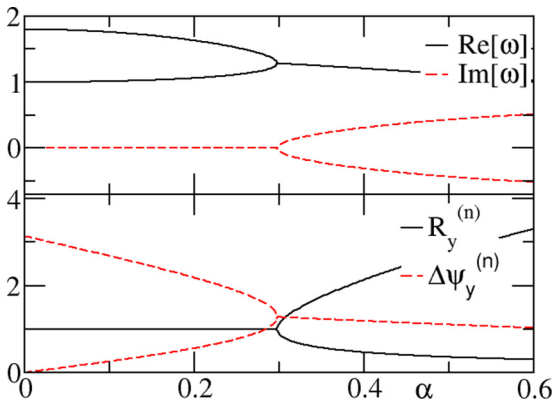

FIG. 2. (Color online) (top) Parametric evolution of the eigenfrequencies of the $\mathcal{PT}$-symmetric ferromagnetic dimer shown in Fig. 1(a). The parameters used are such that $\omega_K = 0.4\omega_H$. (bottom) The same as in (a), but now for the magnitude of the ratio between the y components of the normal modes and their associated phase difference. The same behavior also holds for the x components.

$|\omega| \propto \sqrt{\alpha - \alpha_{\rm cr}}$. This behavior can be exploited in sensing technologies since it enhances the sensitivity of frequency splitting detection (for an optics proposal see Ref. [26]).

Next, we evaluate the normal modes of the ferromagnetic dimer. Using Eqs. (5) and (6) we first evaluate $\vec{\Delta},\vec{\mu}$ and from there extract the original variables $\vec{m}_n$. This yields

$$\begin{pmatrix} m_{1x}^{(l)} \\ m_{1y}^{(l)} \\ m_{2x}^{(l)} \\ m_{2y}^{(l)} \end{pmatrix} = \begin{pmatrix} \frac{\alpha(\omega_H+\omega_K) \pm i\sqrt{\omega_K^2 - \alpha^2\omega_H(\omega_H+2\omega_K)}}{(1+i\alpha)\omega_K} \\ \frac{i\left[\alpha(\omega_H+\omega_K) \pm i\sqrt{\omega_K^2 - \alpha^2\omega_H(\omega_H+2\omega_K)}\right]}{(1+i\alpha)\omega_K} \\ -i \\ 1 \end{pmatrix}, \quad (8)$$

where the subindexes x,y refer to the x,y components of the magnetization vectors and the superindex $l = 1,2$ refers to the normal mode corresponding to the plus and minus signs on the right-hand side of Eq. (8), respectively. $\mathcal{PT}$-symmetry considerations require that in the exact phase, in contrast to the broken one, these vectors are also eigenvectors of the $\mathcal{PT}$ operator. In other words, the ratio of the magnitudes of the relevant components $R_x^{(l)} \equiv |\frac{m_{1x}^{(l)}}{m_{2x}^{(l)}}|, R_y^{(l)} \equiv |\frac{m_{1y}^{(l)}}{m_{2y}^{(l)}}|$ in the exact phase is unity, indicating that the magnitude of the magnetization eigenvectors is the same in both the loss side and the gain side of the dimer. As α becomes larger than $\alpha_{\rm cr}$, the magnitudes of the magnetization in the loss and the gain sides become unequal, indicating that the magnetization eigenmodes reside on either the gain side or the lossy side of the dimer. This behavior can be seen nicely in Fig. 2 (bottom), where we plot $R_y^{(l=1,2)}$ as well as the relative phase difference $\Delta\psi_y^{(l=1,2)}$ between the y components of the $l = 1,2$ modes. We see that for $\alpha = 0$ the phase difference assumes the values $\Delta\psi_y^{(l=1)} = 0$ and $\Delta\psi_y^{(l=2)} = \pi$, indicating symmetric ($\vec{m}_1 = \vec{m}_2$, corresponding to the soft mode) and antisymmetric ($\vec{m}_1 = -\vec{m}_2$, corresponding to the hard mode) combinations. At $\alpha = \alpha_{\rm cr}$ we have a degeneracy of the eigenvectors.

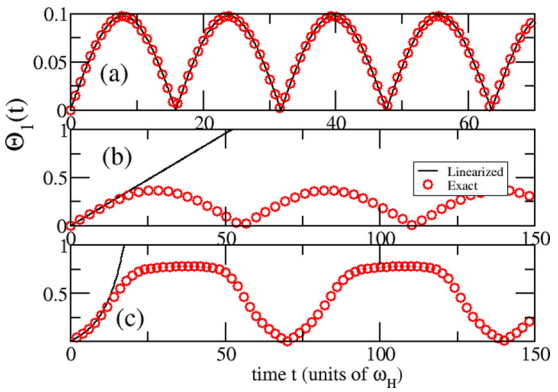

FIG. 3. (Color online) Time dependence of the polar angle $\Theta_1(t)$ associated with the magnetization vector of lossy film. The initial conditions in all cases are $\Theta_1(t=0)=0=\Phi_1(t=0)$ and $\Theta_2(t=0)=0.05, \Phi_2(t=0)=\pi/2$ while $\omega_K=0.4\omega_H$. The results of the exact dynamics equation (2) are indicated with red circles, while the dynamics generated by the linearized equations (3) are indicated with a black line. (a) Exact phase for $\alpha=0.85\alpha_{\rm cr}$. (b) Dynamics at the exceptional point, i.e., $\alpha=\alpha_{\rm cr}$. (c) Broken phase with $\alpha=1.1\alpha_{\rm cr}$. Time is measured in units of inverse ω_H.

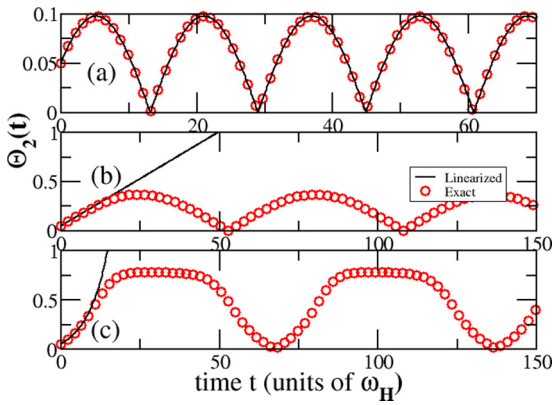

FIG. 4. (Color online) Time dependence of the polar angle $\Theta_2(t)$ associated with the magnetization vector of "gain" film. The initial conditions and parameters are the same as the ones used in Fig. 3. Time is measured in units of inverse ω_H.

B. Nonlinear time evolution

The $\mathcal{PT}$-symmetric nature of the dimer is also encoded in the time evolution of the magnetization vectors and the realization of new types of steady states. The precession dynamics is better represented in spherical coordinates, i.e., switching to the angular variables $\Theta_{1,2}$ and $\Phi_{1,2}$,

$$\begin{aligned} M_{nx} &= M_0 \sin(\Theta_n)\cos(\Phi_n), \\ M_{ny} &= M_0 \sin(\Theta_n)\sin(\Phi_n), \\ M_{nz} &= M_0 \cos(\Theta_n). \end{aligned} \tag{9}$$

These variables are particularly convenient for studying the dynamics because they unveil the fact that there are only two (and not three) independent dynamical variables for each magnetic moment. Specifically, we concentrate on the temporal evolution of the polar angles $\Theta_n(t)$ with respect to the direction of the internal magnetic fields $\vec{H}_n$ (z direction). These polar angles are related to the z components of the magnetic moments. The dynamics of the transverse components is less interesting (just a rapid precession), and it is encoded in the azimuthal angle Φ_n.

In the case of a single film, where only dissipative mechanisms are taken into account, Θ_n decreases due to energy losses, so that the magnetization vectors align with the $\hat{z}$ direction. Conversely, in the presence of only amplification mechanisms, the magnetization of a single film is driven away from the $\hat{z}$ direction.

In the case of $\mathcal{PT}$-symmetric configurations, where a dissipative and an amplified film are coupled together, the resulting dynamics depends on the value of the gain and loss parameter α. Below we present exact numerical solutions of Eqs. (2) for various cases.

When $\alpha<\alpha_{\rm cr}$ [exact phase, see Figs. 3(a) and 4(a)], despite the fact that the dimer is non-Hermitian, the polar angles Θ_n oscillate around the initial misalignment from the $\hat{z}$ axis without being amplified or attenuated, indicating the existence of a new type of steady state. In this domain the linearized equations (3) describe well the exact dynamics (2).

In the broken phase $\alpha>\alpha_{\rm cr}$ [see Figs. 3(c) and 4(c)], the evolution generated by the linearized equations (3) indicates an exponential growth of Θ_n [black lines in Figs. 3(c) and 4(c)] which is associated with the fact that the eigenfrequencies are acquiring an imaginary part. In other words, in this domain, the linear solution is unstable, and the linear approximation is inadequate to describe the dynamics. This exponential growth is eventually suppressed by nonlinear effects which are inherent in the original LLG equations (2). A (numerically exact) solution of the nonlinear problem for Θ_1 as a function of time is shown in Fig. 3(c) by red circles [a similar behavior is observed for Θ_2; see Fig. 4(c)]. This solution corresponds to the initial conditions $\Theta_1(t=0)=0=\Phi_1(t=0), \Theta_2(t=0)=0.05$, and $\Phi_2(t=0)=\pi/2$, and it is periodic in time. We have checked that the period slightly depends on the choice of the initial conditions. In all cases, however, we find a stable periodic solution with no sign of any "runaway" effects.

Similar behavior is observed at the transition point corresponding to $\alpha=\alpha_{\rm cr}$, with the alteration that the linearized equations (3) lead to a linear growth of the polar angles Θ_n [see Figs. 3(b) and 4(b)]. This behavior is a consequence of the EP degeneracy, which results in defective eigenmodes. The particular solution in Figs. 3(b) and 4(b) corresponds to the initial conditions $\Theta_1(t=0)=0=\Phi_1(t=0)$ and $\Theta_2(t=0)=0.05, \Phi_2(t=0)=\pi/2$. We conclude therefore that the linear approximation, which is applicable only in the case for which $\Theta_n \ll 1$, fails to describe the actual dynamics when $\alpha=\alpha_{\rm cr}$.

Finally, we point out that we have checked numerically that the behavior of the angular variables $\Theta_{1,2}$ as discussed above and shown in Figs. 3 and 4 is typical and it is qualitatively the same for other choices of initial conditions.

IV. IN-PLANE GEOMETRY

For completeness we also analyze the in-plane geometry shown in Fig. 1(b). Following the same program as above, we can linearize the LLG equations (under the condition $\vec{h}_{\rm ext}=0$) and study the dynamics of magnetization vectors

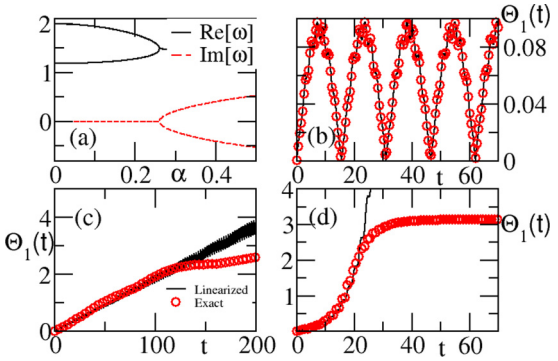

FIG. 5. (Color online) In an in-plane geometry [Fig. 1(b)] for $\omega_K = 0.4\omega_H$ and $\omega_M = 0.4\omega_H$, (a) the parametric evolution of eigenfrequencies vs the gain-loss parameter α and the temporal evolution of $\Theta_1(t)$ in (b) the exact phase with $\alpha = 0.85\alpha_{\rm cr}$, (c) EP with $\alpha = \alpha_{\rm cr}$, and (d) the broken phase with $\alpha = 1.1\alpha_{\rm cr}$. The initial conditions and lines and symbols are the same as in Fig. 3. Time is measured in units of inverse ω_H.

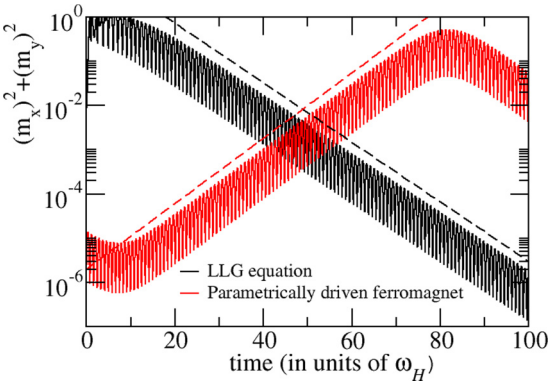

FIG. 6. (Color online) The temporal behavior of the magnetization $m_x^2 + m_y^2$ of a dissipative (black line) and an amplified (red) ferromagnet where gain is introduced via parametric driving. The driving parameters in the last case are such that the amplification increment has equal magnitude but opposite sign with respect to the lossy ferromagnet. The dashed lines are drawn in order to guide the eye and indicate that the ratios in these two cases are the same. The time is measured in units of inverse ω_H.

$\vec{m}_n$. For this geometry the equations for $\vec{m}_n$ differ from Eq. (3) by an additional term $\omega_M m_{nx}\hat{y}$ on the right-hand side where $\omega_M = 4\pi\gamma M_0$:

$$\frac{d\vec{m}_1}{dt} = (\omega_H + \omega_K)\hat{z}\times\vec{m}_1 - \omega_K\hat{z}\times\vec{m}_2 + \omega_M m_{1x}\hat{y} + \alpha\hat{z}\times\frac{d\vec{m}_1}{dt},$$
$$\frac{d\vec{m}_2}{dt} = (\omega_H + \omega_K)\hat{z}\times\vec{m}_2 - \omega_K\hat{z}\times\vec{m}_1 + \omega_M m_{2x}\hat{y} - \alpha\hat{z}\times\frac{d\vec{m}_2}{dt}. \quad (10)$$

These equations enable one to calculate the normal modes of the system as well as the linear dynamics. We have also obtained a solution of the full nonlinear problem for the in-plane geometry. Some representative results are reported in Fig. 5, showing a behavior qualitatively similar to that for the out-of-plane configuration.

V. REALIZATION OF GAIN IN FERROMAGNETIC LAYERS

In this section we would like to point out two possible ways to achieve amplification (gain) of the magnetic oscillations in ferromagnets.

A. Parametric driving

Let us first recall the phenomenon of the parametric resonance of a harmonic oscillator [27]. Consider an oscillator whose eigenfrequency is modulated in time so that the equation of motion is

$$\ddot{x}(t) + \omega_0^2[1 + \eta\cos(2\omega_0 t)]\,x(t) = 0 \quad (\eta \ll 1). \quad (11)$$

The approximate solution of this equation is

$$x(t) = a(t)\sin(\omega_0 t) + b(t)\cos(\omega_0 t), \quad (12)$$

where the slowly varying amplitudes $a(t)$,$b(t)$ grow exponentially with time, with an increment $(\eta\omega_0/4) = \lambda \ll \omega_0$. Thus, the parametrically driven oscillator exhibits an instability (gain). The equilibrium solution $x(t) = 0$ of Eq. (11) is unstable; that is, an infinitesimal deviation from equilibrium results in exponential growth. This growth, on top of rapid oscillations with frequency ω_0, can be modeled by the equation

$$\ddot{x}(t) - 2\lambda\dot{x}(t) + \omega_0^2 x(t) = 0. \quad (13)$$

This exponential growth $\exp(\lambda t)$ is eventually limited by nonlinear effects.

A similar phenomenon occurs for a magnetic moment driven by an appropriate external magnetic field. Consider the in-plane geometry with the external field

$$\vec{H}_{\rm ext} = \left[H_{\rm ext}^{(0)} + h_{\rm ext}(t)\right]\hat{z} \quad (14)$$

in the $\hat{z}$ direction (in the plane of the film), where the weak, time-dependent component can be written as $H_{\rm ext}^{(0)}\eta f(t)$. The geometry when the dc and ac external fields are parallel to one another is known as longitudinal (or parallel) pumping. Such pumping can lead to the excitation of spin waves, with a wavelength smaller than the size of the sample [28]. We, however, are interested only in the uniform magnetization of the entire sample.

Since $\vec{h}_{\rm ext}$ is in the same direction as $H_{\rm ext}^{(0)}$ (which is also in the direction of the equilibrium magnetization $\vec{M}_0$), it cannot cause the ordinary precession of the magnetic moment about the $\hat{z}$ direction. Rather, it can cause an instability via a mechanism analogous to the parametric driving of a harmonic oscillator (see Fig. 6). Indeed, neglecting for the moment the losses, the linearized Landau-Lifshitz equations read

$$\dot{m}_x = -\omega_H[1 + \eta f(t)]\,m_y,$$
$$\dot{m}_y = \omega_H[1 + \eta f(t)]\,m_x + \omega_M m_x, \quad (15)$$

where $\omega_H = \gamma H_0$, $\omega_M = 4\pi\gamma M_0$. (Recall that in this geometry the internal field $H_0 = H_{\rm ext}^{(0)}$). We do not pursue a detailed analysis of Eq. (15) and note only that for the case $\omega_M \gg \omega_H$ the second equation in (15) reduces to $\dot{m}_y = \omega_M m_x$, which,

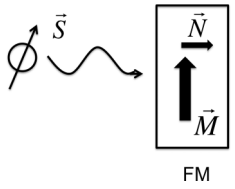

FIG. 7. A beam of spin-polarized electrons impinges on a ferromagnetic layer (FM) with magnetic moment $\vec{M}$.

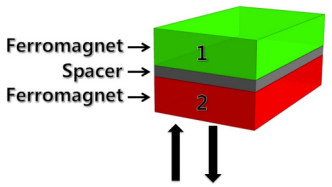

FIG. 8. (Color online) Spin-polarized electrons (up-pointing arrow) impinge on the ferromagnetic layer and are reflected back (down-pointing arrow). Spin angular momentum (but no electric current) is flowing into the layer, creating gain. The red layer indicates the gain ferromagnet, while the green layer indicates the lossy ferromagnet.

after taking a time derivative and substituting $\dot{m}_x$ from the first equation in (15), yields $\ddot{m}_y = -\omega_H\omega_M[1+\eta f(t)]m_y$. For $f(t) = \cos(2\omega_0 t)$, with $\omega_0 = \sqrt{\omega_H\omega_M}$, this coincides with Eq. (11) for the parametrically driven oscillator. Thus, a magnetic moment, parametrically driven with an ac magnetic field, parallel to the constant field Eq. (14), exhibits an instability, i.e., an exponential growth of the precession angle Θ about the $\hat{z}$ direction, limited only by nonlinearity. Such an instability is modeled by reversing the sign of the attenuation term in the Landau-Lifshitz (Gilbert) equation.

Finally, the analysis can be extended to include a decay term into the Landau-Lifshitz equations in a way similar to the inclusion of weak friction in Eq. (11) for the oscillator [27] (see Fig. 6).

B. Spin-transfer torque

A different mechanism for achieving amplification of the magnetic moment precession is based on the spin-transfer phenomenon (see Ref. [29] for a pedagogical review). When spin-polarized electrons are scattered on a ferromagnetic layer, they generally transfer some angular momentum to the layer, thus inducing a torque $\vec{N}$ on the magnetic moment $\vec{M}$ (see Fig. 7). (Spin polarization is usually achieved by passing current through another ferromagnetic layer, a "spin polarizer," not shown in the figure.) Two conditions should be satisfied for the spin transfer to take place: First, the scattering amplitudes must be spin dependent, i.e., must be different for spin-up (parallel to $\vec{M}$) and spin-down electrons (such a difference is provided by the exchange splitting between the minority and majority spin bands in the ferromagnet). Second, the polarization direction of the incident spins $\vec{S}$ should not be strictly parallel to the direction of $\vec{M}$. The angular momentum, transmitted to the ferromagnetic layer by the stream of polarized electrons, affects the dynamics of the magnetic moment $\vec{M}$. The effect is described by an amplification term in the Landau-Lifshitz equation. This term has the same form as the damping term but with an opposite sign (the resulting equation is referred to as the Landau-Lifshitz-Gilbert-Slonczewski equation).

It is interesting to note that spin transfer can occur even in the case of total reflection, provided that the reflection amplitudes for up and down spins, $r_{\rm up} = \exp(i\phi_{\rm up})$ and $r_{\rm down} = \exp(i\phi_{\rm down})$, have different phases [see Eq. (14) in Ref. [29]]. Although the "transmitted" wave in this case is purely evanescent, so that no charge current can flow into the layer, the angular momentum transmitted to the layer is not zero [29,30]. This might provide the most practical way for producing gain in a $\mathcal{PT}$-symmetric magnetic structure (see Fig. 8). Again, as in Fig. 7, we do not show explicitly the setup which produces the spin-polarized current that impinges on the lower film (gain) of our $\mathcal{PT}$-symmetric device. One can find the full setup in Ref. [30].

VI. CONCLUSIONS

In conclusion, we have introduced the notion of $\mathcal{PT}$ symmetry in magnetic nanostructures. Using two coupled ferromagnetic layers, one with loss and another with an equal amount of gain, we demonstrated the emergence of a new type of steady-state dynamics in which the polar angle, although not a constant of motion, is bounded and neither attenuates (as in the case of losses) nor amplifies (as in the case of gain). This non-Hermitian steady state can be reached for values of the gain and loss parameter α that are below a critical value $\alpha_{\rm cr}$. At $\alpha = \alpha_{\rm cr}$ the system experiences an exceptional-point degeneracy where both eigenvalues and eigenvectors of the linearized LLG equations are simultaneously degenerate. It will be interesting to extend this study to the case of spin waves (magnons) and to investigate the possibility of observing phenomena such as magnonic coherent perfect absorbers/lasing, invisibility, etc. [19,20].

ACKNOWLEDGMENTS

We are grateful to V. Vardeny for attracting our interest to the subject. This research was partially supported by AFOSR MURI Grant No. FA9550-14-1-0037 and by Grants No. NSF ECCS-1128571 and No. DMR-1306984. (B.S) acknowledges a Global Initiative grant from Wesleyan University (dean's office).

[1] D. D. Stancil and A. Prabhakar, *Spin Waves: Theory and Applications* (Springer, New York, 2009).

[2] J. Akerman, Science **308**, 508 (2005); S. Datta and B. Das, Appl. Phys. Lett. **56**, 665 (1990).

[3] C. D. Stanciu, F. Hansteen, A. V. Kirilyuk, A. Tsukamoto, A. Itoh, and T. Rasing, Phys. Rev. Lett. **99**, 047601 (2007); J. Stöhr, H. C. Siegmann, A. Kashuba, and S. J. Gamble, Appl. Phys. Lett. **94**, 072504 (2009).

[4] A. V. Nazarov, H. S. Cho, J. Nowak, S. Stokes, and N. Tabat, Appl. Phys. Lett. **81**, 4559 (2002); S. Ghionea, P. Dhagat, and A. Jander, IEEE Sens. J. **8**, 896 (2008).
[5] J. A. Katine and E. E. Fullerton, J. Magn. Magn. Mater. **320**, 1217 (2008).
[6] N. Engheta and R. W. Ziolkowski, *Metamaterials: Physics and Engineering Explorations* (Wiley, Hoboken, NJ, 2006); L. Solymar and E. Shamonina, *Waves in Metamaterials* (Oxford University Press, New York, 2009).
[7] C. Caloz and T. Itoh, *Electromagnetic Metamaterials: Transmission Line Theory and Microwave Applications* (Wiley, Hoboken, NJ, 2006).
[8] P. Deymier, *Acoustic Metamaterials and Phononic Crystals*, Springer Series in Solid-State Sciences Vol. 173 (Springer, Berlin, 2013).
[9] K. G. Makris, R. El-Ganainy, D. N. Christodoulides, and Z. H. Musslimani, Phys. Rev. Lett. **100**, 103904 (2008); Z. H. Musslimani, K. G. Makris, R. El-Ganainy, and D. N. Christodoulides, *ibid.* **100**, 030402 (2008).
[10] C. Ruter, K. Makris, R. El-Ganainy, D. Christodoulides, M. Segev, and D. Kip, Nat. Phys. **6**, 192 (2010).
[11] A. Regensburger, C. Bersch, M.-A. Miri, G. Onishchukov, D. N. Christodoulides, and U. Peschel, Nature (London) **488**, 167 (2012).
[12] J. Schindler, Z. Lin, J. M. Lee, H. Ramezani, F. M. Ellis, and T. Kottos, J. Phys. A **45**, 444029 (2012); H. Ramezani, J. Schindler, F. M. Ellis, U. Gunther, and T. Kottos, Phys. Rev. A **85**, 062122 (2012).
[13] M. C. Zheng, D. N. Christodoulides, R. Fleischmann, and T. Kottos, Phys. Rev. A **82**, 010103 (2010).
[14] H. Ramezani, T. Kottos, R. El-Ganainy, and D. N. Christodoulides, Phys. Rev. A **82**, 043803 (2010); F. Nazari, N. Bender, H. Ramezani, M. K. Moravvej-Farshi, D. N. Christodoulides, and T. Kottos, Opt. Express **22**, 9574 (2014).
[15] N. Bender, S. Factor, J. D. Bodyfelt, H. Ramezani, D. N. Christodoulides, F. M. Ellis, and T. Kottos, Phys. Rev. Lett. **110**, 234101 (2013).
[16] B. Peng, S. K. Ozdemir, F. Lei, F. Monifi, M. Gianfreda, G. L. Long, S. Fan, F. Nori, C. M. Bender, and L. Yang, Nat. Phys. **10**, 394 (2014).
[17] L. Feng, Y.-L. Xu, W. S. Fegadolli, M.-H. Lu, J. E. B. Oliveira, V. R. Almeida, Y.-F. Chen, and A. Scherer, Nat. Mater. **12**, 108 (2013).
[18] Z. Lin, J. Schindler, F. M. Ellis, and T. Kottos, Phys. Rev. A **85**, 050101 (2012).
[19] Z. Lin, H. Ramezani, T. Eichelkraut, T. Kottos, H. Cao, and D. N. Christodoulides, Phys. Rev. Lett **106**, 213901 (2011).
[20] S. Longhi, Phys. Rev. A **82**, 031801 (2010); Y. D. Chong, L. Ge, and A. D. Stone, Phys. Rev. Lett. **106**, 093902 (2011).
[21] A. Guo, G. J. Salamo, D. Duchesne, R. Morandotti, M. Volatier-Ravat, V. Aimez, G. A. Siviloglou, and D. N. Christodoulides, Phys. Rev. Lett. **103**, 093902 (2009).
[22] In the most general case, as the control parameter increases, the system can experience multiple "phase transitions" where the spectrum changes from real to complex.
[23] C. M. Bender, Rep. Prog. Phys. **70**, 947 (2007).
[24] E. M. Graefe, H. J. Korsch, and A. E. Niederle, Phys. Rev. Lett. **101**, 150408 (2008); M. Hiller, T. Kottos, and A. Ossipov, Phys. Rev. A **73**, 063625 (2006); M. K. Oberthaler, R. Abfalterer, S. Bernet, J. Schmiedmayer, and A. Zeilinger, Phys. Rev. Lett. **77**, 4980 (1996).
[25] X. Zhu, H. Ramezani, C. Shi, J. Zhu, and X. Zhang, Phys. Rev. X **4**, 031042 (2014); R. Fleury, D. Sounas, and A. Alu, Nat. Commun. **6**, 5905 (2015).
[26] J. Wiersig, Phys. Rev. Lett. **112**, 203901 (2014).
[27] L. D. Landau and E. M. Lifshitz, *Mechanics*, 3rd ed., Course of Theoretical Physics Vol. 1 (Pergamon, Oxford, UK, 1976).
[28] A. G. Gurevich and G. A. Melkov, *Magnetization Oscillations and Waves* (CRC Press, Florida, USA, 1996).
[29] D. C. Ralph and M. D. Stiles, J. Magn. Magn. Mater. **320**, 1190 (2008).
[30] K. Xia, P. J. Kelly, G. E. W. Bauer, A. Brataas, and I. Turek, Phys. Rev. B **65**, 220401(R) (2002).